The dynamics of electronic energy transfer in novel multiporphyrin functionalized dendrimers: A time-resolved fluorescence anisotropy

ARTICLE · MARCH 2000

CITATIONS
36

READS
7

7 AUTHORS, INCLUDING:

Joost N H Reek
University of Amsterdam
386 PUBLICATIONS **10,791** CITATIONS
SEE PROFILE

Maxwell J. Crossley
University of Sydney
261 PUBLICATIONS **5,694** CITATIONS
SEE PROFILE

Aw Bosman
SupraPolix
40 PUBLICATIONS **2,862** CITATIONS
SEE PROFILE

Albertus P H J Schenning
Technische Universiteit Eindhoven
295 PUBLICATIONS **14,360** CITATIONS
SEE PROFILE

ARTICLES

The Dynamics of Electronic Energy Transfer in Novel Multiporphyrin Functionalized Dendrimers: A Time-Resolved Fluorescence Anisotropy Study

Edwin K. L.Yeow and Kenneth P. Ghiggino*

Photophysics Laboratory, School of Chemistry, The University of Melbourne, Parkville, Victoria 3052, Australia

Joost N. H. Reek† and Maxwell J. Crossley

School of Chemistry, The University of Sydney, NSW 2006, Australia

Anton W. Bosman, Albert P. H. J. Schenning, and E. W. Meijer

Laboratory of Macromolecular and Organic Chemistry, Eindhoven University of Technology, P.O. Box 513, 5600 MB Eindhoven, The Netherlands

Received: September 1, 1999; In Final Form: December 15, 1999

The dynamics of electronic energy transfer (EET) for a series of spherical porphyrin arrays based on different generations of poly(propylene imine) dendrimers have been investigated using time-resolved fluorescence anisotropy measurements (TRAMS) in a glass environment. The first, third, and fifth generation dendrimers consisting of 4, 16, and 64 porphyrin chromophores, respectively, are investigated in this study. We observe a depolarization of the fluorescence in all three dendrimers as compared to the monoporphyrin model compound, indicating that EET takes place between the chromophores within the dendrimers. The experimental TRAMS results were compared to computationally simulated data obtained from the Pauli master equation. For the first generation dendrimer, we find the rate of energy transfer is well described by Förster theory. Anomalous behavior is observed in the third generation dendrimer where the limiting anisotropy value suggests that energy transfer is confined to only the porphyrins contained within a dendron. Interdendron porphyrin EET is thus unfavorable due to dendron segregation. In the fifth generation dendrimer, the TRAMS data is best explained by a model which includes independent and simultaneous rapid EET between porphyrins contained on the surface of the dendrimer sphere and slow EET between porphyrins in adventitious dendrons found probably either outside or inside of the sphere.

1. Introduction

A special class of hyperbranched, three-dimensional molecular structures known as dendrimers has attracted considerable attention in recent years.[1−5] The controlled synthesis of dendrimers results in their size and architecture being both regular and well-defined. Such unique physical properties have given rise to several important applications for these novel macromolecules. In particular, dendrimers are now recognized to have important roles in guest−host chemistry,[6] catalysis,[7] optical electronics,[8] analytical chemistry,[3] biology[9] and medicine.[10]

Recently, many studies have been focused on using dendrimers to mimic the photosynthetic light-harvesting antennae system.[11−15] Kopelman and co-workers[11] have considered the kinetics of excitation energy trapping from an initially excited state on a phenylacetylene dendrimer to a trap located at its center. An energy gradient created along the linear phenylacetylene chain was found to facilitate the funneling of the excitation energy.[11,12,16,17] Jiang and Aida[13] have also examined the cooperation of dendron subunits in aryl ether dendrimer porphyrins for energy transduction. More recently, we have synthesized and reported a series of novel spherical porphyrin arrays based on different generations of poly(propylene imine) dendrimers.[18] The morphologies of these molecules resemble that of the photosynthetic light harvesting antenna LH2 system and have thus created interest as artificial photosynthetic devices.

In this paper, we investigate the dynamics of electronic energy transfer (EET) for our multiporphyrin funtionalized dendrimers, G*n*P*m*, where *n* is the generation number and *m* is the number of porphyrin end-groups (see Chart 1), using time-resolved fluorescence anisotropy measurements (TRAMS). This technique not only yields information on the dynamics of energy transfer but also provides a tool to study the structural properties of the dendrimers.[19,20] TRAMS involves the measurement of the fluorescence intensity decay profiles through a polarizing analyzer element arranged in a parallel and perpendicular orientation with respect to the polarization of the excitation light.

* Corresponding author. E-mail: k.ghiggino@chemistry.unimelb.edu.au.
† Present address: Institute of Molecular Chemistry, University of Amsterdam, Nieuwe Achtergracht 166, 1018 WV, Amsterdam, The Netherlands.

10.1021/jp993116u CCC: $19.00
Published on Web 03/04/2000

When emission occurs from a chromophore before EET, that emission will be polarized with a specific direction relative to the direction of the polarized excitation light. As the excitation undergoes some energy transfer steps to other chromophores of different orientation, each of these steps will incur some changes in the polarization of the emitted light, hence giving rise to a depolarization of the fluorescence emission.[21,22]The most commonly invoked singlet−singlet EET mechanism between two chromophores (D and A) is the Coulombic interaction described by Förster theory.[23] Equation 1 gives the Förster's rate of energy transfer between *D* and *A* separated by a distance *R*,

$$k = \left(\frac{1}{\tau_D}\right)\left(\frac{R_O}{R}\right)^6 \tag{1}$$

where τ_D is the fluorescence lifetime of the donor D in the absence of the acceptor A and R_o is the critical distance between the two molecules such that the energy transfer probability equals the emission probability and is defined by

$$R_O^6 = \frac{9000(\ln 10)\kappa^2\phi_D J(\bar{\nu})}{128\pi^5 N\eta^4} \tag{2}$$

where ϕ_D is the fluorescence quantum yield of the donor, N is Avogadro's number, η is the refractive index of the solvent, κ^2 is the orientation factor, and $J(\bar{\nu})$ is the spectral overlap integral of the emission of D with the absorption of A. This term is easily calculated from experimentally obtainable absorption and emission spectra via equations 3 and 4

$$J(\bar{\nu}) = \int_0^\infty \epsilon(\bar{\nu}) f(\bar{\nu}) \frac{d\bar{\nu}}{\bar{\nu}^4} \tag{3}$$

where $\epsilon(\bar{\nu})$ is the molar absorbance of the acceptor at frequency $\bar{\nu}$ and $f(\bar{\nu})$ is the normalized fluorescence spectrum of the donor defined by

$$f(\bar{\nu}) = \frac{F(\bar{\nu})}{\int_0^\infty F(\bar{\nu})d\bar{\nu}} \tag{4}$$

where $F(\bar{\nu})$ represents the emission intensity per unit frequency. This mechanism is developed from a framework based on Coulombic dipole−dipole interaction between chromophores. Other mechanisms such as the short-range orbital-dependent interactions (e.g., Dexter-type interaction[24] and through-configuration interaction[25]) and the superexchange coupling[26] have previously been discussed by two of the authors.[22,27]

To obtain a complete understanding of the effects of the dendrimer's size on EET dynamics, we have chosen to investigate three generations of the porphyrin functionalized dendrimers G*n*P*m*. Namely, the first (G1P4), third (G3P16), and fifth (G5P64) generation dendrimers consisting of 4, 16, and 64 porphyrin chromophores, respectively. Because of the bulky porphyrin end-groups, back-folding is not possible. Thus for G1P4 it is assumed that the chromophores are distributed along the perimeter of a circular disk with radius 12 Å, while for the higher generation dendrimers G3P16 and G5P64 the porphyrins are assumed to be randomly arranged on the surface of a sphere with radius 16.2 and 22 Å, respectively. The radii of the dendrimers were estimated by taking the sum of the radius of the porphyrin molecule and the radius of gyration of the poly(propylene imine) dendrimers determined from a molecular dynamics study.[28]

When excitation energy is localized on the chromophores, the energy transfer among the porphyrin molecules is best modeled using the Pauli master equation.[22] Because of their globular shape, dendrimers are often seen to be analogous to spherical micelles whose photophysics and energy transfer dynamics are well-characterized.[29−33] In particular, Turro et al.[34] have employed such a model to effectively study the luminescence quenching of $[Ru(phen)_3]^{2+}$ by $[Co(phen)_3]^{3+}$ bound to the surface of starbust dendrimers. It will be shown that for the G*n*P*m* dendrimers the EET dynamics inadvertently become more complex as the generation number increases. For our purpose, we have developed three different models, one for each generation of the dendrimers, to explain the EET dynamics. These models ranging from the Monte Carlo method to the two-particle approximation will be considered in greater detail in the following section. The theoretically derived time-resolved fluorescence anisotropy decay profiles are then compared to the experimental results to provide insights into the energy transfer dynamics for our molecular systems.

This paper is organized as follows: The experimental procedures are outlined in section 2. The general theoretical model based on the Pauli master equation is introduced in section 3 before the Monte Carlo method and the two-particle approximation are discussed. In section 4, the models developed are applied to the porphyrin functionalized dendrimers and the results compared to the experimental data. Finally, the conclusion is presented in section 5.

2. Experimental Method and Data Treatment

2.1. Experimental Method. The synthesis of the porphyrin functionalized dendrimers and the monoporphyrin model compound G0P1 (Chart 1) have been described elsewhere.[18] Solutions of all compounds were prepared in ethanol-isopentane-diethyl ether (EPA) solvent to absorbances of less than 0.2 at 595 nm for both steady-state and time-resolved fluorescence measurements. The samples were thoroughly degassed by repeated freeze−pump−thaw cycles to remove any dissolved gases before being cooled to a glassy state and maintained at 77 K using a variable liquid nitrogen cryostat (Oxford Instruments Optistat). The study of the samples in a frozen glass is necessary to eliminate any fluorescence depolarization caused by molecular rotation. Steady-state fluorescence measurements were recorded on a Spex Fluorolog 2 spectrofluorimeter.

The time-resolved fluorescence lifetimes and anisotropy were measured using the time-correlated single photon counting method.[35] The excitation source is a synchronously mode-locked Rhodamine 6G dye laser (Spectra Physics 3500) which provided excitation pulses of ca. 5 ps fwhm at a repetition rate of 4 MHz. An excitation wavelength of 595 nm was used. Fluorescence lifetime measurements were recorded by observing the emission through a polarizer set at the magic angle (54.7°) relative to the vertically polarized excitation light. For fluorescence anisotropy measurements, the parallel ($I_{||}(t)$) and perpendicular ($I_{\perp}(t)$) decay profiles were measured by monitoring fluorescence through a rotatable polarizer oriented parallel and perpendicular to the vertically polarized excitation beam. The fluorescence decays were detected with a microchannel plate photomultiplier tube (Hamamatsu model R2809U-01) after passing through a polarization scrambler and a single grating monochromator (Jobin Yvon H-10). The $I_{||}(t)$ and $I_{\perp}(t)$ profiles were collected in two 512 channel memories of a multichannel analyzer (MCA). To account for laser intensity fluctuations, both the direction of the rotatable polarizer and the MCA memories were switched with dwell times of 30 s for 90 cycles. Emission was

CHART 1 . Structures of the first generation (G1P4), third generation (G3P16), and fifth generation (G5P64) dendrimers together with the monoporphyrin model compound (G0P1).

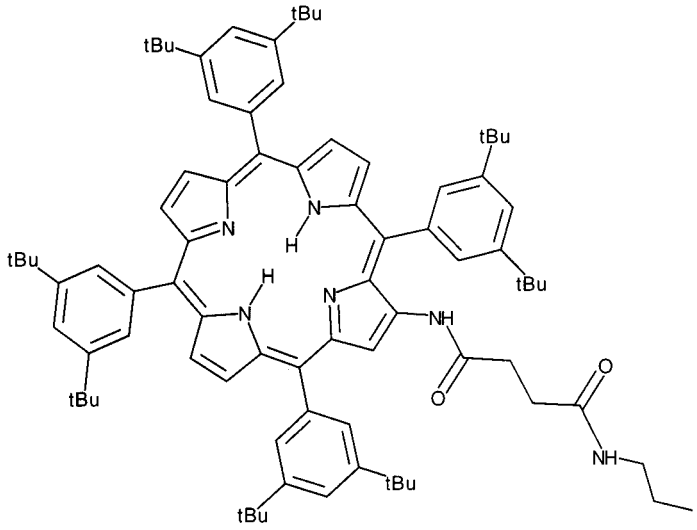

G0P1

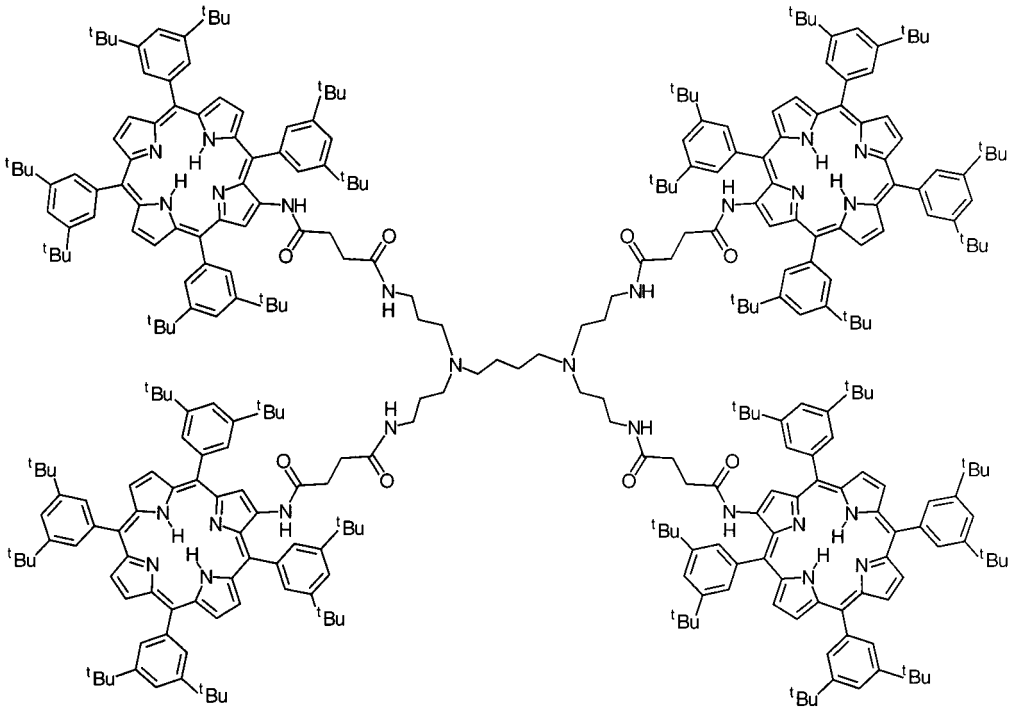

G1P4

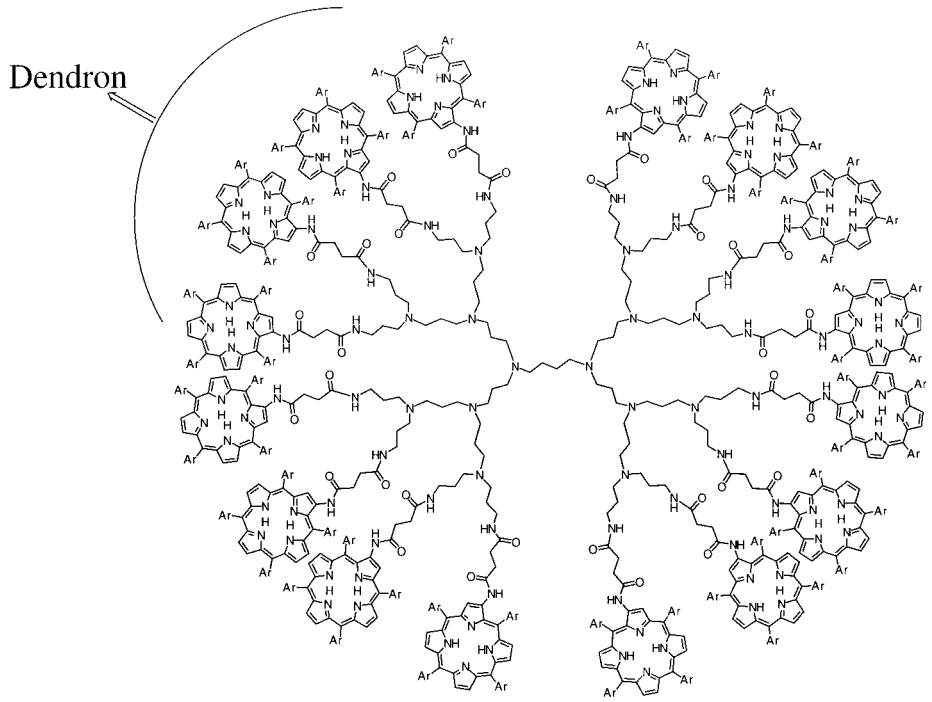

G3P16

G5P64

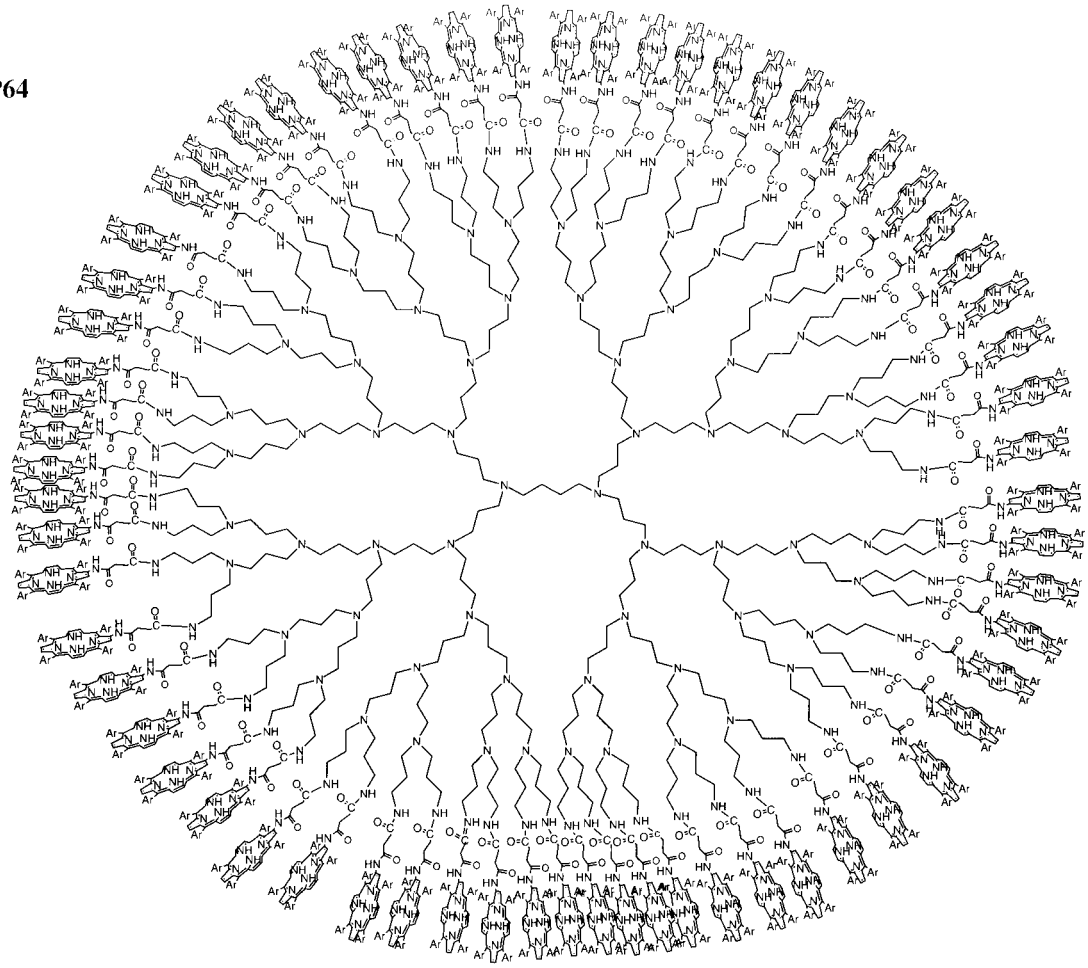

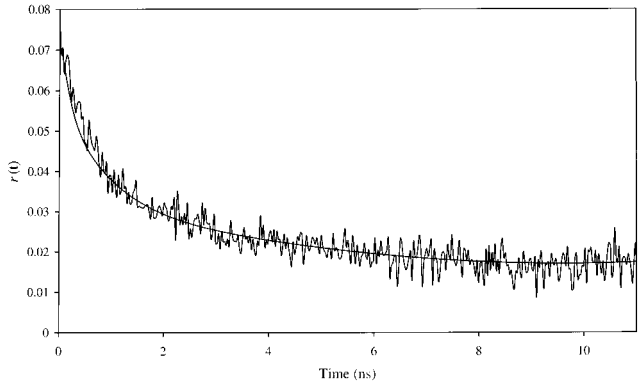

Figure 1. Fluorescence anisotropy decay of G1P4 and the anisotropy fit (solid line) obtained by deconvoluting $I_{||}(t)$ and $I_{\perp}(t)$ in terms of arbitrary four exponential fits.

monitored at 655 nm. The collected data were then analyzed using the nonlinear least-squares iterative reconvolution procedures based on the Marquardt algorithmn.[35] Fluorescence anisotropy profiles were constructed using the following expression:

$$r(t) = \frac{I_{||}(t) - I_{\perp}(t)}{I_{||}(t) + 2I_{\perp}(t)} \tag{5}$$

Since there is no molecular rotation in the rigid low-temperature glass, any time-dependent change in fluorescence anisotropy should arise only from energy transfer.

2.2. Data Treatment. The effects of the finite instrument response on $r(t)$ are small due to its narrow width and lack of substructure. To support this claim, both the $I_{||}(t)$ and $I_{\perp}(t)$ decay profiles for G1P4 were deconvoluted separately in terms of arbitrary four-exponential fits.[35] The resulting time-resolved fluorescence anisotropy ($r(t)$), free of convolution effects, was subsequently generated from eq 5. An excellent fit to the experimental data was obtained as shown in Figure 1. Therefore, all anisotropy decays in this work were generated without deconvolution. The time zero, t_0, was estimated by first matching the rising edge of both the polarized decays and the instrument response function and then choosing t_0 to be the time taken for the instrument reponse to peak.[29(b)]

3. Models for Electronic Energy Transfer

3.1. Pauli Master Equation. Given a multichromophoric system consisting of N identical chromophores, the time-dependent probability of an excitation residing on chromophore i, $P_i(t)$, is described by the Pauli master equation[36]

$$\frac{dP_i(t)}{dt} = \sum_{j=1}^{N} w_{ij}[P_j(t) - P_i(t)] \tag{6}$$

where w_{ij} is the Förster excitation energy transfer rate between molecules i and j. The formal solution of the above equation is given by eq 7

$$\boldsymbol{P}(t) = \boldsymbol{G}(t)\boldsymbol{P}(0) \tag{7}$$

where $\mathbf{G}(t)$ is the Green's function normally expressed in terms of the eigenvalues (λ) and eigenvectors ($\boldsymbol{M}$) of eq 6

$$\boldsymbol{G}(t) = \boldsymbol{M}\exp(\lambda t)\,\boldsymbol{M}^{-1} \tag{8}$$

and $\boldsymbol{P}(0)$ is the initial distribution of excitation. The matrix element of the Green's function in the site representation $G_{ij}(t)$ is the conditional probablity that chromophore i is excited at time t given that chromophore j was initially excited. The eigenvalues and eigenvectors needed to compute the Green's function elements were obtained using the EISPACK[37] matrix eigensystem routines, and the inverse matrix, $\boldsymbol{M}^{-1}$, was computed using the LINPACK[38] subroutines.

When the chromophores are randomly oriented, the time-resolved fluorescence anisotropy, $r(t)$, of the multichromophoric system is given by the probability that the initially excited chromophore is still excited at time t.[39] Note that since we are considering a homogeneous system, each chromophore has an equal probablity of being initially excited. In this case,[40a]

$$r(t) = \frac{\sum_{i}^{N} G_{ii}(t)}{N} r_{\mathrm{O}} \tag{9}$$

where r_o is the anisotropy of the model compound (i.e., the fundamental anisotropy in the absence of energy transfer or molecular rotation). At long times, energy transfer between molecules distributed randomly in a *finite* volume results in an equalization of excitation probability among all chromophores.[29,39b,40a,b] Detailed calculations[40c] on a pair of randomly oriented chromophores have shown that the anisotropy contribution from the indirectly excited molecule is small and can be assumed to be zero. Therefore, for a *finite* system, the excitation probability after many energy hops would be equally distributed among N chromophores such that the residual anisotropy (r_∞) is r_o/N.[29c,40a,b] Valeur et al.[40a,b] have reported energy transfer and long-time leveling off of the emission anisotropy at $r_o/7$ for a cyclodextrin system labeled with seven randomly oriented naphthoyloxy chromophores.

In the first generation dendrimer, where the separations between the porphyrins are assumed to be fixed, a single set of interchromophoric distances is considered. Equation 9 describes the ensemble average anisotropy for G1P4, in which the orientations of the porphyrin transition dipoles are uncorrelated and random.[40a] For the higher generation dendrimers, several configurations (c), each with a different set of interchromophoric distances and energy transfer rates, are taken into account whereby the contribution from each configuration to the ensemble average anisotropy must now be considered.[40a] This will be discussed in the following subsection.

3.2. Monte Carlo Method. As discussed in the Introduction, the porphyrin chromophores are assumed to be randomly distributed around the spherical surface of the higher generation dendrimers. The coordinates of the porphyrin molecules can therefore be sampled using the Monte Carlo method. A molecular dynamics study has previously shown that dendron (monomers belonging to different primary branches) segregation exists in poly(propylene imine) based dendrimers.[28] This means that dendrons do not overlap and simply occupy their own individual surface area.[28,41] For G3P16, the four porphyrin chromophores within a dendron are thus randomly distributed on the surface of a quarter of a sphere with radius 16.2 Å.

The spherical coordinates of each porphyrin chromophores in a dendron of G3P16 are given by $[r_i,\theta_i,\varphi_i]$. The radial component, r_i, is fixed to the radius of the dendrimer while the two independent variables (θ_i and φ_i) must be specified. The polar angle θ_i and the azimuthal angle φ_i can have values in the range of $[0 \le \theta_i \le \pi/2]$ and $[0 \le \varphi_i \le \pi]$, respectively. To avoid a high and unrealistic concentration of chromophores at the poles of the sphere, we adopt the approach of Fayer and

co-workers.[29(c)] In this case, the polar angle θ is distributed according to the normalized distribution $H(\theta')$

$$H(\theta') = \sin\theta' \tag{10}$$

such that

$$\int_0^{\pi/2}\sin(\theta')\mathrm{d}\theta' = 1 \tag{11}$$

Using the inverse transform method,[42] we have

$$\zeta = \int_0^{\theta}\sin(\theta')\mathrm{d}\theta' \tag{12}$$

where ζ is a uniformly distributed random number. Solving eq 12 gives eq 13 which generates random variable θ distributed according to eq 10

$$\theta = \cos^{-1}[1-\zeta] \tag{13}$$

On the other hand, the azimuthal angle φ is simply calculated from eq 14

$$\varphi = \pi\zeta \tag{14}$$

The spherical coordinates of the chromophores are then subsequently transformed to Cartesian coordinates via eq 15

$$\begin{aligned} x &= r\sin\theta\cos\varphi \\ y &= r\sin\theta\sin\varphi \\ z &= r\cos\theta \end{aligned} \tag{15}$$

and the respective Förster's rate constant between chromophores obtained from eqs 1−4. The dynamics of energy transfer in a configuration is again described by the Pauli master equation (eq 6). To obtain a *configurationally averaged* $\langle r(t)\rangle$ value,[40a] 10 000 configurations were generated and

$$\langle r(t)\rangle = \frac{\sum_c\sum_i^4 G_{ii}(t)}{4c} r_{\mathrm{O}} \tag{16}$$

where c is the number of configurations (i.e., 10 000). All computations in this work were carried out in a Cray J916 computer.

3.3. Two-Particle Approximation. For the sake of comparison with the Monte Carlo method, we shall use the two-particle approximation[43] to derive $\langle P_n(t)\rangle$ the configurationally averaged probability of finding at time t the excitation still remaining on the initially excited chromophore when surrounded by n acceptors. When two chromophores are separated by a distance of r_j, the distance distribution function, $\varpi(r_j)$, is defined to be the probability of finding the acceptor at a distance between r_j and $r_j + dr_j$ from the donor. For a sphere of radius $\hat{R}$ with randomly oriented chromophores on the surface

$$\varpi(r_j) = K\frac{r_j}{\hat{R}^2} \tag{17}$$

where K is the normalization constant. When $\tilde{r}$ is the minimum separation between the porphyrin chromophores found in a dendron of the third generation dendrimer (G3P16), we get

$$K = \frac{\hat{R}^2}{\left(\hat{R}^2 - \frac{\tilde{r}^2}{2}\right)} \tag{18}$$

and

$$\int_{\tilde{r}}^{\sqrt{2}\hat{R}}\varpi(r_j)\mathrm{d}r_j = 1 \tag{19}$$

The displacement r_j can be expressed in terms of the angular separation between the two chromophores ϕ_j (see Figure 2) to give[44]

$$r_j = \sqrt{2}\hat{R}(1-\cos\phi_j)^{1/2} \tag{20}$$

For the donor−acceptor pair, the time-dependent probability of the excitation residing on the donor ($E_j(t)$) due to the presence of an acceptor at site j is given by the solution of the Pauli master equation (eq 6)[43]

$$E_j(t) = \frac{1}{2}\{1 + \exp[-2tw(r_j)]\} \tag{21}$$

where $w(r_j)$ is the Förster EET rate constant between the donor and the acceptor. On averaging $E_j(t)$ over the distance distribution of the acceptor chromophore (eq 17), one obtains

$$\langle E_j(t)\rangle = \frac{1}{2}\int_{\tilde{r}}^{\sqrt{2}\hat{R}}\{1 + \exp[-2tw(r_j)]\}\varpi(r_j)\mathrm{d}r_j \tag{22}$$

and

$$\langle E_j(t)\rangle = \frac{K}{2}\int_{\mathscr{T}}^{\pi/2}\left\{1 + \exp\left[-\frac{2t}{\tau_{\mathrm{D}}}\left(\frac{R_{\mathrm{O}}^2}{2\hat{R}^2(1-\cos\phi_j)}\right)^3\right]\right\}\sin\phi_j\mathrm{d}\phi_j \tag{23}$$

where

$$\mathscr{T} = \cos^{-1}\left(1 - \frac{\tilde{r}^2}{2\hat{R}^2}\right) \tag{24}$$

when eqs 1, 17, and 20 are invoked. Writing $(1 - \cos\phi_j) = \alpha$, we can recast eq 23 into the convenient form given in eq 25

$$\langle E_j(t)\rangle = \frac{K}{2}\int_{\mathscr{T}}^{1}[1 + \exp(-\upsilon t\,\alpha^{-3})]\mathrm{d}\alpha \tag{25}$$

where

$$\mathscr{T} = \frac{\tilde{r}^2}{2\hat{R}^2} \tag{26}$$

and

$$\upsilon = \frac{1}{4\tau_{\mathrm{D}}}\left(\frac{R_0}{\hat{R}}\right)^6 \tag{27}$$

Now, the two-particle approximation can be applied when $\langle E_j(t)\rangle$ is assumed to be unaffected by the existence of the other $(n-1)$ acceptor chromophores found at some other positions. The configurationally averaged $\langle P_n(t)\rangle$ is therefore a product of the independent two-particle decay $\langle E_j(t)\rangle$

$$\langle P_n(t)\rangle = \langle E_j(t)\rangle^n \tag{28}$$

It is important to note that eq 28 derived from eq 25 correctly describes the EET dynamics during short times but asymptoti-

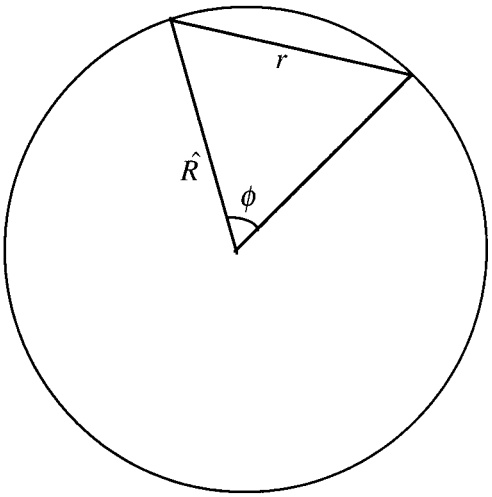

Figure 2. Diagram of the assumed two-particle geometry on a spherical surface. $\hat{R}$ is the radius of the sphere, r and ϕ are the linear and angular separations between the particles.

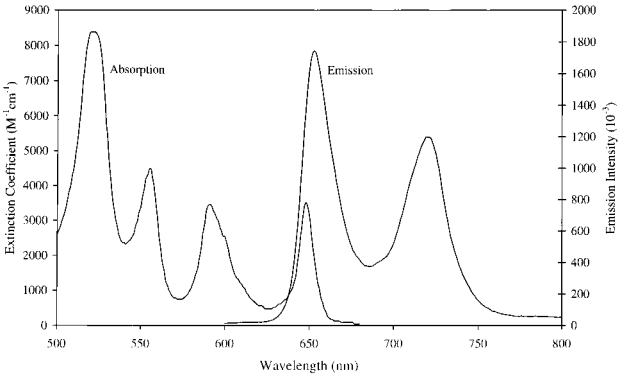

Figure 3. Absorption and emission spectra of G0P1 in EPA at 77 K.

cally converges to a value of $[K(1 - \mathcal{T})/2]^n$ rather than the correct value of $1/(n + 1)$ at infinite time when the excitation energy is equally distributed among the $(n + 1)$ chromophores. To overcome this discrepancy, the Padé approximant[45] is used to approximate the term $\exp(-\upsilon t\ \alpha^{-3})$ in eq 25 before the integration is performed numerically. This procedure retains the dynamics of the energy transfer at short times and forces $\langle P_n(t)\rangle$ to approach $1/(n + 1)$ at infinite times thus correcting for the asymptotic behavior. This will be further illustrated in the next section.

4. Results and Discussion

4.1. The Model Compound G0P1 and the First Generation Dendrimer G1P4. Fluorescence emission and absorption spectra were measured for the monoporphyrin model compound, G0P1 (Figure 3). Efficient resonance energy transfer occurs when there is a significant overlap between the emission and absorption spectra of the porphyrin chromophores.[46] From Figure 3, we note that there is a substantial amount of spectra overlap such that the calculated value for the spectra overlap integral, $J(\bar{\nu})$, is 1.2×10^{-14} M^{-1} cm^3. If the porphyrin molecules in the dendrimers are not close enough to effect short-range orbital-overlap dependent interaction, and if superexchange coupling is negligible, then the dominant EET mechanism is the Förster Coulombic dipole−dipole interaction.

The time-resolved fluorescence anisotropy of G0P1 measured at an emission wavelength of 655 nm when excited at 595 nm

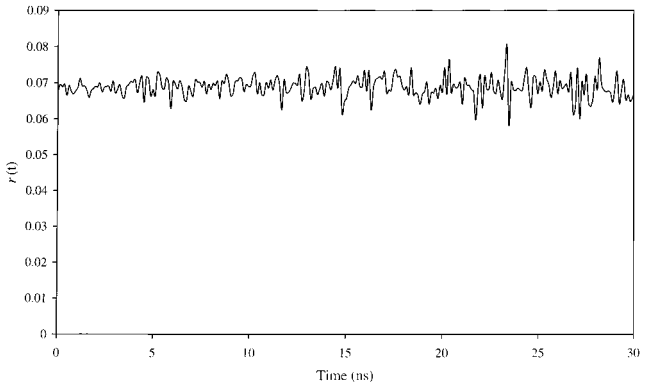

Figure 4. Time-resolved fluorescence anisotropy of G0P1 in glassy solution of EPA at 77 K with $\lambda_{excitation} = 595$ nm and at $\lambda_{emission} = 655$ nm.

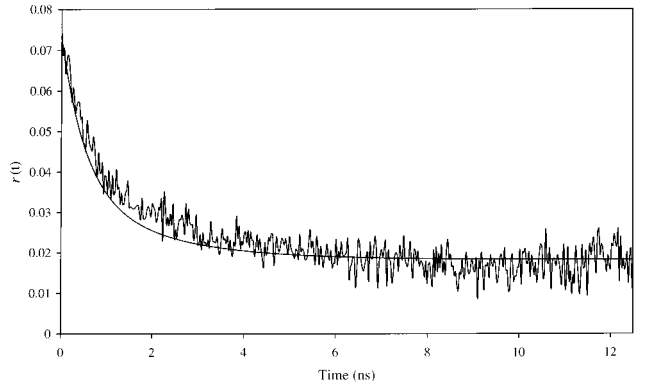

Figure 5. Time-resolved fluorescence anisotropy of G1P4 in glassy solution of EPA at 77 K with $\lambda_{excitation} = 595$ nm and at $\lambda_{emission} = 655$ nm. The theoretical anisotropy (solid line) describes the EET dynamics as depicted in Figure 6.

remains reasonably constant ($r_O \approx 0.07$) throughout the observed time range (Figure 4). Steady-state fluorescence excitation anisotropy of tetraphenylporphyrin also reflects a similar value when excited at the same wavelength.[47] The observation that the initial anisotropy is not 0.4 indicates that mixed polarization transitions are involved in fluorescence from porphyrins. Gouterman[47] has shown that the intensity of the $Q_x(1\leftarrow 0)$ band arises from vibrational mixing with the intense Soret bands which introduces both *x*- and *y*-polarized intensity to the Q-band. The absence of an anisotropy decay for the model compound is expected since no time-dependent depolarization process should occur in the rigid glass.

Let us examine now the fluorescence anisotropy decay curve of G1P4 when excited at 595 nm in a rigid solvent (see Figure 5). It is observed that the anisotropy profile decays before leveling off to a residual anisotropy value of $r_\infty = 0.0175$. This indicates that excitation energy is transferred between the porphyrin molecules and eventually becomes equally distributed among the four chromophores (i.e., $r_\infty = r_O/4$), confirming random spatial orientation between the chromophores.[40a,b] Rather than consider the oversimplified picture of a single energy transfer rate between adjacent porphyrin molecules, we assume that the chromophores are arranged along the perimeter of a circular disk with radius 12 Å such that the interchromophore separations are no longer constant as depicted in Figure 6. Here, the C_2 symmetric G1P4 has chromophores found at the corners of an enclosed rectangle where the nearest separation between the porphyrins is 15 Å and the furthest displacement is equivalent to the diameter of the circular disk (i.e., 24 Å). At such separations, short-range orbital-dependent interaction can

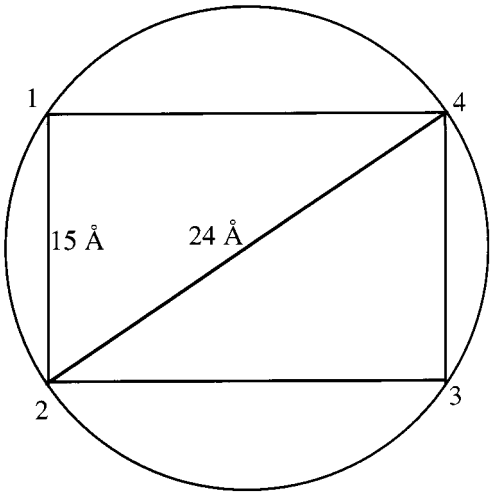

Figure 6. Schematic representation for G1P4 with porphyrins (labeled 1, 2, 3, and 4) located at the corners of an enclosed rectangle. The shortest and longest porphyrin−porphyrin distances are 15 and 24 Å, respectively.

be neglected and the corresponding Förster's rate of energy transfer between any two chromophores can be calculated from eq 1 with $\tau_D = 14.5$ ns and R given in Figure 6. The orientation factor, κ^2, for the randomly oriented porphyrins in a rigid glass equals 0.476.[48] The critical distance, R_o, determined for the porphyrin functionalized dendrimers is 22.62 Å given further that $\phi_D = 0.09$[49] and $\eta_{EPA} = 1.3545$. The computationally simulated anisotropy decay obtained from the Pauli master equation (eq 6) and eq 9 is in good agreement with the experimental results (see Figure 5). Our proposed model describing the EET dynamics in G1P4 is promising and provides an indication of the structure of the first generation dendrimer. A point worth mentioning is that contrary to the first generation *N*-*t*-BOC-protected glycine functionalized dendrimer (DAB-*dendr*-(NH-Gly-*t*-BOC)$_4$),[50] the theoretical investigation here does not suggest in general that the end-group porphyrins in G1P4 are assembled on one side of the molecule while the core atoms are positioned on the other side. This is probably because of the steric effects of the bulky terminal groups which prevent such a conformation from being feasible even though H-bonding is present in G1P4.

Another frequently encountered mode of EET is the directed (or dispersive) energy transfer.[51] This arises from spectral inhomogeneous broadening caused by the variation of the solvation shell structure of each chromophore which leads to a statistical distribution of the frequencies of the electronic transition.[52,53] In several inhomogeneously broadened systems of chemically similar chromophores, directed energy transfer from the "blue" centers to the "red" centers occurs to an extent where impeded EET[51] and lack of depolarization[54] at the long-wavelength edge of the absorption spectrum were observed. This was first reported by Weber[55] (Weber's red-edge effect) and recently by many other groups.[51,54,56,57] In particular, Valeur et al.[54] have observed an increase in the steady-state excitation anisotropy at the vibronic red-edge of a multichromophoric cyclodextrin. A study reported by Zenkevich et al.[58] on the existence of spectral inhomogeneity for porphyrin macromolecules has therefore prompted us to investigate the presence of vibronic red-edge effects in the first generation porphyrin functionalized dendrimer. The anisotropy decay for G1P4 obtained when excited at 610 nm, the red-edge of the $Q_x(1\leftarrow0)$ vibronic band, is shown in Figure 7. The observed increased in

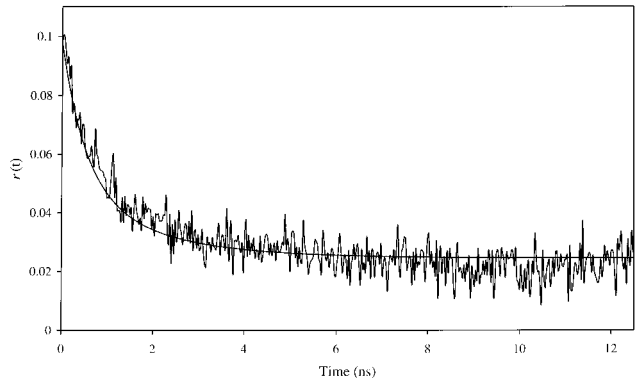

Figure 7. Time-resolved fluorescence anisotropy of G1P4 in glassy solution of EPA at 77 K with $\lambda_{excitation} = 610$ nm and at $\lambda_{emission} = 655$ nm. The theoretical anisotropy (solid line) is obtained as explained in the text.

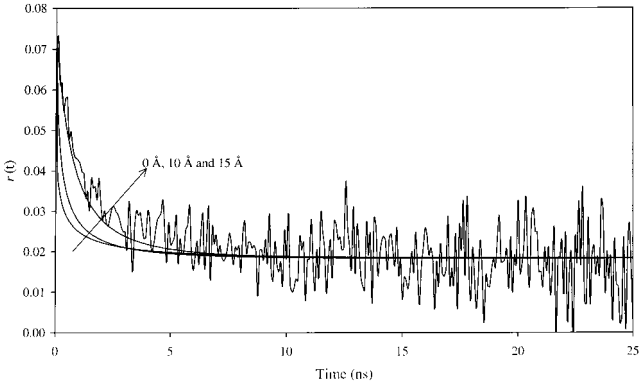

Figure 8. Time-resolved fluorescence anisotropy of G3P16 in glassy solution of EPA at 77 K with $\lambda_{excitation} = 595$ nm and at $\lambda_{emission} = 655$ nm. Comparison with Monte Carlo calculations (solid lines) for minimum interchromophoric separations of 0, 10, and 15 Å.

the residual anisotropy, $r_\infty = 0.0245$ (cf. $r_\infty \approx 0.0175$ for excitation wavelength at 595 nm), can either be a consequence of the higher fundamental anisotropy or directed energy transfer. Using the same interchromophoric energy transfer rates as discussed above (Figure 6), we note that the theoretical anisotropy decay curve agrees well with the experimental data (Figure 7). This leads us to believe that the effects of inhomogeneous broadening at 77 K on the energy transfer dynamics for the porphyrin functionalized dendrimers studied here are small.

4.2. The Third Generation Dendrimer G3P16. Figure 8 shows the time-resolved fluorescence anisotropy curve for the third generation dendrimer, G3P16, which reveals that the residual anisotropy value is not the expected 0.0044 ($r_\infty \approx r_O/16$) attained when an equilibrium distribution of excitation on each of the randomly oriented sixteen chromophores is achieved. Instead, $r_\infty \approx 0.0175$ (cf. the residual anisotropy for G1P4) which suggests that EET is essentially confined to only the four porphyrins contained within a dendron. The rather long and flexible branching units would enable each dendron and associated porphyrins to be randomly arranged on a quarter of the dendrimer's spherical surface. We can thus employ the Monte Carlo method as discussed in section 3.2 to assign the coordinates of the chromophores. The theoretical anisotropy decays obtained from eq 16 for three different minimum interchromophoric separations (i.e. $\tilde{r} = 0$, 10, and 15 Å) are also presented in Figure 8. Only for $\tilde{r} = 15$ Å is the energy

transfer dynamics well described by the theoretical model. Hence, the maximum rate of EET is 0.81 ns^{-1}.

To complement the above findings, we turn to the two-particle approximation developed in section 3.3. The relevant equations (28 and 25) were shown to misbehave only at long times. To correct for the asymptotic value of $\langle P_n(t)\rangle$, it is therefore necessary to use the Padé approximant to approximate $\exp(-vt\ \alpha^{-3})$ in eq 25. In this case, for $\tilde{r} = 15$ Å, the [2,1] Padé approximant about $x = \alpha^{-3} = 21/25$ was used

$$\exp(-vt\ \alpha^{-3}) = \frac{\exp\left(-\frac{vt21}{25}\right)}{2}\left\{\frac{[6 - 4vt(x - 21/25) + (vt)^2(x - 21/25)^2]}{[3 + vt(x - 21/25)]}\right\} \quad (29)$$

The resulting two-particle approximation anisotropy decay is given in Figure 9 along with the experimental result. Again, a good agreement is seen which confirms the validity of the Monte Carlo method; namely that the porphyrins within a dendron are randomly arranged on the surface of a quarter of the third generation dendrimer. Since the Förster's rate constant (eq 1) is inversely proportional to R^6, only interchromophoric distances smaller than the critical distance R_o play a major role in energy transfer. Thus, the probability for EET from a donor molecule to an acceptor molecule decreases rapidly when their separation approaches R_o and is negligible beyond that.[59] When we assume, for simplicity, the average conformation of a dendron has porphyrins located at the corners of a rectangle with minimum and maximum separations $R = 15$ Å ($k = 0.81$ ns^{-1}) and 22.62 Å ($k = 0.069$ ns^{-1}) respectively, the enclosed area of the four chromophores is only 31% of a quarter of the dendrimer's surface area. Together with the presence of dendron segregation, this implies that the porphyrins found in different dendrons are too far apart (i.e., ≥ critical distance) to effect any favorable electronic coupling to assist EET.

4.3. The Fifth Generation Dendrimer G5P64. A complex anisotropy decay is observed for the fifth generation dendrimer, G5P64 (see Figure 10). It is worthwhile to note some interesting features of the $r(t)$ profile which will shed light on both the EET dynamics and the structure of the macromolecule. A very rapid initial anisotropy decay occurs to a value of $r(t) \approx 0.015$ (at $t = 4$ ns) before gradually regaining intensity and leveling off at $r_\infty \approx 0.018$. These features allude to complex energy transfer dynamics which cannot be easily explained using the models proposed earlier for the lower generation dendrimers. This unusual behavior can be explained as follows. The "dip" and "rise" in the anisotropy curve suggest that there are more than one species in the system whose contributions to the effective $r(t)$ are different with time. This is easily followed from polarization addition law which states that the effective anisotropy is given by[60]

$$r(t) = \frac{\sum_{i=1}^{N} r_i(t)I_i(t)}{\sum_{i=1}^{N} I_i(t)} \quad (30a)$$

$$= \sum_{i=1}^{N} f_i(t)r_i(t) \quad (30b)$$

where N is the total number of independent species, $r_i(t)$ and

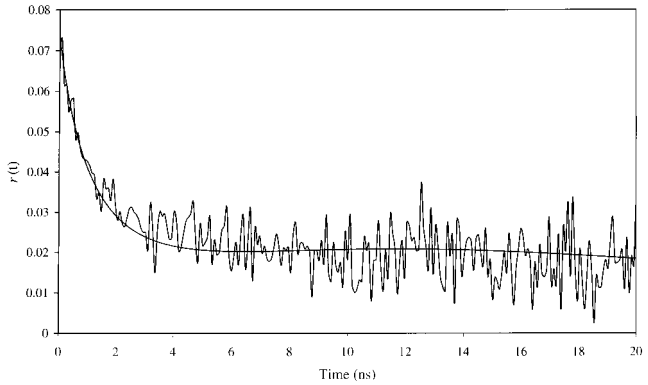

Figure 9. Comparison of experimental anisotropy for G3P16 with two-particle approximation calculations.

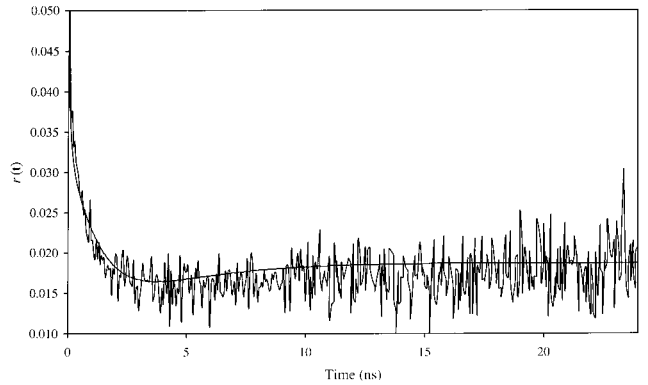

Figure 10. Time-resolved fluorescence anisotropy of G5P64 in glassy solution of EPA at 77 K with $\lambda_{excitation} = 595$ nm and at $\lambda_{emission} = 655$ nm. Comparison with theoretical simulation of $r(t)$ (solid line) as described in the text.

$I_i(t)$ are the anisotropy decay and intensity contributions by the ith species to the effective anisotropy and the total intensity, respectively, and $f_i(t)$ is the ith fraction of the total intensity. The lifetime decay for G5P64 measured at 77 K was fitted satisfactorily only to a triple exponential function with lifetimes of 0.64, 2.44, and 12.5 ns and corresponding preexponential factors of 15263, 10619 and 13277. The two short lifetimes (τ_1 and τ_2) can be attributed to relatively strong couplings between porphyrins (i.e., the superradiance effect),[61,62] whereas the longest lifetime component τ_3, close to the lifetime of the model compound, was assigned to porphyrins with much weaker interchromophoric interactions. Thus, in G5P64, there are in general two contributing species to the effective anisotropy. The first species (core porphyrins) are closely packed together such that strong couplings are experienced which ultimately give rise to the two short lifetimes and are revealed in the rapid initial anisotropy decay and a small blue shift and broadening of the absorption band[63] when compared to the model compound (Figure 11). Their total contributions to $r(t)$ are important at short times but diminish rapidly (i.e., $f_i(\infty)r_i(\infty) \rightarrow 0$) when $r(t)$ regains intensity at longer times due to the second contributing species, porphyrins with the long lifetime component (i.e., adventitious porphyrins). The residual anisotropy clearly suggests that EET occurs only between four adventitious porphyrins which are too distant from the core chromophores to allow any effective energy transfer. A simple model is used here to illustrate the EET dynamics. We assume that 56 core porphyrins adopt a circular arrangement with a uniform interchromophore separation of 9 Å ($k = 17.4$ ns^{-1}) while each of the four adventitious chromophores are 18 Å ($k = 0.27$ ns^{-1}) apart. Equation 30b is rewritten as

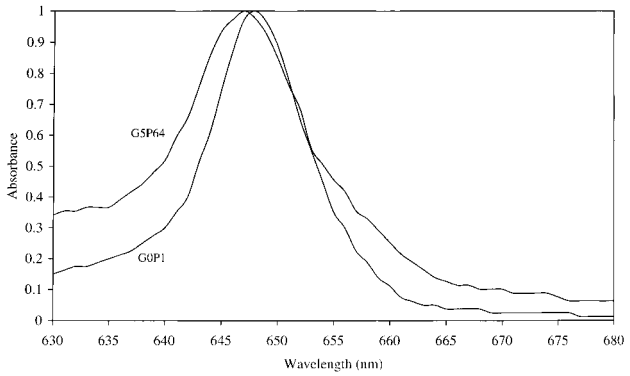

Figure 11. Absorption spectra of G0P1 and G5P64 at 77 K.

$$r(t) = f_{core}(t)r_{core}(t) + f_{adv}(t)r_{adv}(t) \quad (31)$$

where "core" and "adv" represent core and adventitious porphyrins, respectively, $f_{core}(t) = (I_1(t) + I_2(t))/(I_1(t) + I_2(t) + I_3(t))$, and $f_{adv}(t) = (I_3(t))/(I_1(t) + I_2(t) + I_3(t))$. The two contributing anisotropy factors $r_{core}(t)$ and $r_{adv}(t)$ were computed from the Pauli master equation. The theoretical anisotropy decay obtained from eq 31 is in excellent agreement with the experimental results as shown in Figure 10, and all the anomalous features are present.

From the above discussion, we propose that structural defects may be the cause for such unusual trends. Electrospray mass spectrometry has recently shown that the fifth generation poly(propylene imine) dendrimer consists of molecules which are strucurally imperfect.[64] In particular, one of the more prominent structures has 56 peripheral core porphyrins packed closely (e.g., 9 Å) at the surface of the spherical dendrimer while a dendron of four adventitious porphyrins stops at generation 3 due to a defected growth. The adventitious porphyrins are found in the internal cavity of the dendrimer. As shown by Meijer and coworkers,[6] who encapsulated rose bengal within the internal cavity of a fifth generation poly(propylene imine) dendrimer, there is sufficient space in the dendrimer's interior for the adventitious porphyrins to be relatively far apart from each other (e.g., 18 Å). In the presence of static[62] (i.e., site energy fluctuation) and dynamic[65] (i.e., system-bath interaction) disorders, the collective core porphyrins can be considered to be reduced to a number of (<56) multilevel molecules whose point dipoles are far removed from the adventitious porphyrins. This long separation created between the two species results in inefficient EET. Another possible structure proposed here consists of 56 porphyrins arranged in a similar fashion as above but consisting of two dendrons of adventitious porphyrins located outside the dendrimer's surface. This projection also allows the porphyrins to achieve a "spread-out" conformation.

The unusual "dip" and "rise" behavior for the time-resolved anisotropy decay due to energy transfer within G5P64 is, to the best of our knowledge, reported for the very first time here. We must stress that the rapid EET dynamics between the core porphyrins may be more complex than suggested in our model and is not revealed fully in our experimental data. The ultrafast anisotropy decay is of the order of the time-resolution of the time-correlated photon counting technique used in this work (~80 ps). Nevertheless, the method presented here provides both a valuable means of elucidating the complicated EET dynamics in the fifth generation dendrimer and an insight into the structure of the macromolecule.

5. Conclusion

We have demonstrated that the novel multiporphyrin functionalized dendrimers described here are able to absorb light and efficiently delocalize the excitation energy over the chromophore arrays with minimal loss during the energy migration process. The dendrimers are thus acting as excellent light-harvesting antennae.[66] We have also shown that TRAMS can provide valuable information on the structures of the dendrimers and therefore allow useful insights into the design of more efficient photon harvesting systems.

Acknowledgment. K.P.G. and M.J.C. thank the Australian Research Council (ARC) for financial support of this work. The award of a Melbourne Research Scholarship to E.K.L.Y. is acknowledged. E.K.L.Y. and K.P.G. are grateful to the ORMOND High-Performance Computing facility for use of the Cray J916 computer.

References and Notes

(1) (a) Tomalia, D. A.; Naylor, A. M.; Goddard, W. A., III *Angew. Chem., Int. Ed. Engl.* **1990**, *29*, 138. (b) Dvornic, P. R.; Tomalia, D. A. *Sci. Spectra* **1996**, *5*, 36.

(2) (a) Newkome, G. R.; Moorefield, C. N.; Vögtle, F. *Dendritic Molecules: Concepts, Syntheses, Perspectives*; VCH: Weinheim, 1996. (b) Fischer, M.; Vögtle, F. *Angew. Chem., Int. Ed. Engl.* **1999**, *38*, 884. (c) Newkome, G. R. *Pure Appl. Chem.* **1998**, *70*, 2337.

(3) Matthews, O. A.; Shipway, A. N.; Stoddart, J. F. *Prog. Polym. Sci.* **1998**, *23*, 1.

(4) Smith, D. K.; Diederich, F. *Chem. Eur. J.* **1998**, *4*, 1353.

(5) Bosman, A. W.; Janssen, H. M.; Meijer, E. W. *Chem. Rev.* **1999**, *99*, 1665.

(6) (a) Jansen, J. F. G. A.; Meijer, E. W. *Macromol. Symp.* **1996**, *102*, 27. (b) Jansen, J. F. G. A.; de Brabander-van den Berg, E. M. M.; Meijer, E. W. *Science* **1994**, *266*, 1226.

(7) Stinson, S. C. *Chem. Eng. News* **1997**, *75*, 28.

(8) Atwood, J. L.; Davies, J. E. C.; Macnicol, D. D.; Vögtle, F.; Lehn, J.-M. *Comprehensive Supramolecular Chemistry*; Pergamon Press: Oxford, 1996.

(9) Roberts, J. C.; Bhalgat, M. K.; Zera, R. T. *J. Biomed. Mater. Res.* **1996**, *30*, 53.

(10) Twyman, L. J.; Beezer, A. E.; Esfand, R.; Hardy, M. J.; Mitchell, J. C. *Tetrahedron Lett.* **1999**, *40*, 1743.

(11) (a) Kopelman, R.; Shortreed, M.; Shi, Z.-Y.; Tan, W.; Bar-Haim, A.; Klafter, J. *Phys. Rev. Lett.* **1997**, *78*, 1239. (b) Bar-Haim, A.; Klafter, J.; Kopelman, R. *J. Am. Chem. Soc.* **1997**, *119*, 6197. (c) Shortreed, M. R.; Swallen, S. F.; Shi, Z.-Y.; Tan, W.; Xu, Z.; Devadoss, C.; Moore, J. S.; Kopelman, R. *J. Phys. Chem. B* **1997**, *101*, 6318. (d) Swallen, S. F.; Shi, Z.-Y.; Tan, W.; Xu, Z.; Moore, J. S.; Kopelman, R. *J. Lumin.* **1998**, *76*, *77*, 193.

(12) (a) Bar-Haim, A.; Klafter, J. *J. Phys. Chem. B* **1998**, *102*, 1662. (b) Bar-Haim, A.; Klafter, J. *J. Lumin.* **1998**, *76*, *77*, 197.

(13) Jiang, D.-L.; Aida, T. *J. Am. Chem. Soc.* **1998**, *120*, 10895.

(14) Gilat, S. L.; Adronov, A.; Fréchet, J. M. J. *Angew. Chem., Int. Ed. Engl.* **1999**, *38*, 1422.

(15) (a) Jenkins, R. D.; Andrews, D. L. *J. Phys. Chem. A* **1998**, *102*, 10834. (b) Risser, S. M.; Beratan, D. N.; Onuchic, J. N. *J. Phys. Chem.* **1993**, *97*, 4523.

(16) Tretiak, S.; Chernyak, V.; Mukamel, S. *J. Phys. Chem. B* **1998**, *102*, 3310.

(17) (a) Harigaya, K. *Chem. Phys. Lett.* **1999**, *300*, 33. (b) Harigaya, K. *Phys. Chem. Chem. Phys.* **1999**, *1*, 1687.

(18) Reek. J. N. H.; Bosman, A. W.; Schenning, A. P. H. J.; Ghiggino, K. P.; Yeow, E. K. L.; Meijer, E. W.; Crossley, M. J. (to be submitted to *J. Am. Chem. Soc.*).

(19) Sluch, M. I.; Scheblykin, I. G.; Varnavsky, O. P.; Vitukhnovsky, A. G.; Krasovskii, V. G.; Gorbatsevich, O. B.; Muzafarov, A. M. *J. Lumin.* **1998**, *76*, *77*, 246.

(20) Hofkens, J.; Latterini, L.; De Belder, G.; Gensch, T.; Maus, M.; Vosch, T.; Karni, Y.; Schweitzer, G.; De Schryver, F. C.; Hermann, A.; Müllen, K. *Chem. Phys. Lett.* **1999**, *304*, 1.

(21) Ghiggino, K. P.; Smith, T. A. *Prog. React. Kinet.* **1993**, *18*, 375.

(22) Ghiggino, K. P.; Yeow, E. K. L.; Haines, D. J.; Scholes, G. D.; Smith, T. A. *J. Photochem. Photobiol. A: Chem.* **1996**, *102*, 81.

(23) (a) Förster, Th. *Annalen der Physik* **1948**, *2*, 55. (b) Förster, Th. *Z. Naturforsch.* **1949**, *4a*, 321. (c) Förster, Th. *Discuss. Faraday Soc.* **1959**, *27*, 7. (d) Förster, Th. In *Modern Quantum Chemistry*; Sinanoglu, O., Ed.; Academic Press: New York, 1965; p 93.

(24) Dexter, D. L. *J. Chem. Phys.* **1953**, *21*, 836.
(25) (a) Harcourt, R. D.; Scholes, G. D.; Ghiggino, K. P. *J. Chem. Phys.* **1994**, *101*, 10521. (b) Scholes, G. D.; Harcourt, R. D.; Ghiggino, K. P. *J. Chem. Phys.* **1996**, *104*, 5054.
(26) McConnell, H. M. *J. Chem. Phys*. **1961**, *35*, 508.
(27) Yeow, E. K. L.; Haines, D. J.; Ghiggino, K. P.; Paddon-Row, M. N. *J. Phys. Chem. A* **1999**, *103*, 6517.
(28) Cavallo, L.; Fraternali, F. *Chem. Eur. J.* **1998**, *4*, 927.
(29) (a) Marcus, A. H.; Fayer, M. D. *J. Chem. Phys.* **1991**, *94*, 5622. (b) Marcus, A. H.; Diachun, N. A.; Fayer, M. D. *J. Phys. Chem.* **1992**, *96*, 8930. (c) Finger, K. U.; Marcus, A. H.; Fayer, M. D. *J. Chem. Phys.* **1994**, *100*, 271. (d) Keller, L.; Hussey, D. M.; Fayer, M. D. *J. Phys. Chem.* **1996**, *100*, 10257.
(30) (a) Berberan-Santos, M. N.; Prieto, M. J. E. *J. Chem. Soc., Faraday Trans.* **1987**, *83*, 1391. (b) Berberan-Santos, M. N.; Prieto, M. J. E.; Szabo, A. G. *J. Chem. Soc., Faraday Trans.* **1992**, *88*, 255.
(31) Barzykin, A. V.; Tachiya, M. *J. Chem. Phys.* **1995**, *102*, 3146.
(32) Yekta, A.; Winnik, M. A.; Farinha, J. P. S.; Martinho, J. M. G. *J. Phys. Chem. A* **1997**, *101*, 1787.
(33) Blumen, A.; Klafter, J.; Zumofen, G. *J. Chem. Phys.* **1986**, *84*, 1397.
(34) ben-Avraham, D.; Sculman, L. S.; Bossmann, S. H.; Turro, C.; Turro, N. J. *J. Phys. Chem. B* **1998**, *102*, 5088.
(35) Phillips, D.; O'Connor, D. V. *Time-Correlated Single Photon Counting*; Academic Press: New York, 1983.
(36) Webber, S. E. *Chem. Rev.* **1990**, *90*, 1469.
(37) Smith, B. T.; Boyle, J. M.; Dongarra, J. J.; Moler, B. B.; In *Lecture Notes in Computer Science, Vol 6: Matrix Eigensystem Routines – EISPACK Guide*; Goos, G., Hartmanis, J., Eds.; Springer-Verlag: New York, 1976.
(38) Dongarra, J. J.; Moler, C. B.; Bunch, J. R.; Stewart, G. W. *LINPACK User's Guide*; SIAM: Philadelphia, 1992.
(39) (a) Gochanour, C. R.; Andersen, H. C.; Fayer, M. D. *J. Chem. Phys.* **1979**, *70*, 4254. (b) Ediger, M. D.; Fayer, M. D. *J. Chem. Phys.* **1983**, 78, 2518.
(40) (a) Berberan-Santos, M. N.; Choppinet, P.; Fedorov, A.; Jullien, L.; Valeur, B. *J. Am. Chem. Soc*. **1999**, *121*, 2526. (b) Berberan-Santos, M. N.; Canceill, J.; Gratton, E.; Jullien, L.; Lehn, J.-M.; So, P.; Sutin, J.; Valeur, B. *J. Phys. Chem.* **1996**, *100*, 15. (c) Berberan-Santos, M. N.; Valeur, B. *J. Chem. Phys.* **1991**, *95*, 8048.
(41) Mansfield, M. L. *Polymer* **1994**, *35*, 1827.
(42) Rubinstein, R. Y. *Simulation and the Monte Carlo Method*; John Wiley & Sons: New York, 1981.
(43) Blumen, A. *J. Chem. Phys*. **1980**, *72*, 2632.
(44) (a) Estep, T. N.; Thompson, T. E. *Biophys. J.* **1979**, *26*, 195. (b) Koppel, D. E.; Fleming, P. J.; Strittmatter, P. *Biochemistry* **1979**, *18*, 5450. (c) Eisinger, J.; Blumberg, W. E.; Dale, R. E. *Ann. N.Y. Acad. Sci.* **1981**, *366*, 155.
(45) Graves-Morris, P. R. In *Padé Approximation and Its Applications, Lecture Notes in Mathematics, Vol 765*; Wuytack, L., Ed.; Springer-Verlag: Berlin, 1979.
(46) Guillet, J. *Polymer Photophysics and Photochemistry*; Cambridge University Press: London, 1985.
(47) Gouterman, M.; Stryer, L. *J. Chem. Phys.* **1962**, *37*, 2260.
(48) (a) Hass, E.; Wilchek, M.; Katchalski-Katzir, E.; Steinberg, I. Z. *Proc. Natl. Acad. Sci. U.S.A.* **1975**, *72*, 1807. (b) Dale, R. E.; Eisinger, J. *Proc. Natl. Acad. Sci. U.S.A.* **1976**, *73*, 271.
(49) Gouterman, M. In *The Porphyrins*; Dolphin, D., Ed.; Academic Press: New York, 1978.
(50) Bosman, A. W.; Bruining, M. J.; Kooijman, H.; Spek, A. L.; Janssen, R. A. J.; Meijer, E. W. *J. Am. Chem. Soc.* **1998**, *120*, 8547.
(51) (a) Stein, A. D.; Peterson, K. A.; Fayer, M. D. *Chem. Phys. Lett.* **1989**, *161*, 16. (b) Stein, A. D.; Peterson, K. A.; Fayer, M. D. *J. Chem. Phys.* **1990**, *92*, 5622. (c) Stein, A. D.; Fayer, M. D. *Chem. Phys. Lett.* **1991**, *176*, 159.
(52) Demchenko, A. P. *Ultraviolet Spectroscopy of Proteins*; Springer-Verlag: Berlin, 1986.
(53) Nemkovich, N. A.; Rubinov, A. N.; Tomin, V. I. In *Topics in Fluorescence Spectroscopy*; Lakowicz, J. R., Ed.; Plenum Press: New York, 1991; Vol. 2.
(54) Berberan-Santos, M. N.; Pouget, J.; Valeur, B.; Canceill, J.; Jullien, L.; Lehn, J.-M. *J. Phys. Chem*. **1993**, *97*, 11376.
(55) Weber, G. *Biochem. J*. **1960**, *75*, 335.
(56) Hess, S.; Åkesson, E.; Cogdell, R. J.; Pullerits, T.; Sundström, V. *Biophys. J.* **1995**, *69*, 2211.
(57) Jimenez, R.; Dikshit, S. N.; Bradforth, S. E.; Fleming, G. R. *J. Phys. Chem.* **1996**, *100*, 6825.
(58) Zenkevich, E.; Shul'ga, A.; Chernook, A.; Sagun, E.; Gurinovich, G. *Proc. Indian Acad. Sci. (Chem. Sci.)* **1995**, *107*, 795.
(59) Van der Meer, W. B.; Coker, G.; Chen, S. S.-Y. *Resonance Energy Transfer*; VCH Publisher: New York, 1994.
(60) Dale, R. E.; Eisinger, J. In *Biochemical Fluorescence: Concepts Vol 1*; Chen, R. F., Edelhoch, H., Eds.; Marcel Dekker: New York, 1975.
(61) Scholes, G. D.; Turner, G. O.; Ghiggino, K. P.; Paddon-Row, M. N.; Piet, J. J.; Schuddeboom, W.; Warman, J. M. *Chem. Phys. Lett*. **1998**, *292*, 601.
(62) Fidder, H.; Knoester, J.; Wiersma, D. A. *J. Chem. Phys.* **1991**, *95*, 7880.
(63) Kasha, M.; Rawls, H. R.; Ashraf El-Bayoumi, M. *Pure Appl. Chem.* **1965**, *11*, 371.
(64) Hummelen, J. C.; van Dongen, J. L. J.; Meijer, E. W. *Chem. Eur. J*. **1997**, *3*, 1489.
(65) Potma, E. O.; Wiersman, D. A. *J. Chem. Phys.* **1998**, *108*, 4894.
(66) Gregory Van Patten, P.; Shreve, A. P.; Lindsey, J. S.; Donohoe, R. J. *J. Phys. Chem. B* **1998**, *102*, 4209.